Target-oriented amplitude tomography with joint translational, rotational and strain measurements

Shihao Yuan & Eileen Martin
Center for Wave Phenomena and Dept. of Geophysics, Colorado School of Mines, Golden CO 80401
syuan@mines.edu

ABSTRACT
4D seismic is valuable for hydrocarbon reservoir and CO_2 injection monitoring, and recent advances in sensing technology and data analysis have made it a more affordable tool for planning and operations. We propose a novel, efficient tomography scheme for inverting time-lapse seismic changes within a target region. This method combines target-oriented waveform inversion with various seismic measurements: translational, rotational, and strain data. Unlike full waveform inversion (FWI) and travel-time tomography, it relies on the relative amplitude information between different measurements. We will show that the ratio of amplitudes between translational and strain, or translational and rotational motions, is exclusively sensitive to structural changes near the recording location. This near-receiver sensitivity makes the proposed method resistant to potential repeatability issues during time-lapse surveys and unknown baseline variations outside the target area. We demonstrate the efficiency and accuracy of the proposed method using 2D elastic numerical examples. The results outperform those obtained using conventional target-oriented FWI with only geophone (translational) recordings, even under inaccurate source positions and baseline models.

Key words: Time-lapse, waveform inversion, rotation, strain, target-oriented

1 INTRODUCTION

Many 4D seismic studies focus on changes in the reservoir and its surrounding area, which is typically much smaller than the entire subsurface. Target-oriented waveform inversion, also known as localized inversion, restricts the computational domain to the area of interest, significantly reducing computational costs (Willemsen et al., 2016; Yuan et al., 2021; Biondi et al., 2023). This approach is particularly valuable for time-lapse surveys, where computationally expensive waveform tomography might be needed frequently, such as weekly or monthly. The method assumes knowledge of the background model beforehand, allowing a local solver, such as the wavefield injection method, to replace a global solver with sufficient accuracy. However, discrepancies between the acquired model and ground truth can contribute to misfits between observed and modeled waveforms. This misfit, caused by inaccurate external background models, will inevitably be mapped into the target region during localized tomography and interfere with the true time-lapse structural variations. Besides, non-repeatability issues during time-lapse surveys due to non-permanent acquisitions can contaminate the data and cause artifacts in the estimation of temporal structural changes (Zhou and Lumley, 2021).

To address this limitation, we propose incorporating multiple seismic observables, including translation, rotation, and strain motions, into the wave-equation-based tomography framework. Instead of inverting conventional translational recordings alone, we invert the so-called apparent S-wave speed observables, derived from the amplitude ratio of translation and rotation. Similarly, we invert the apparent P-wave speed observables, formulated as the amplitude ratio of translation and strain. These new combined observables are exclusively focusing on amplitude information and therefore, less sensitive to arrival time inaccuracies. This allows for accurate inversion of local structures without

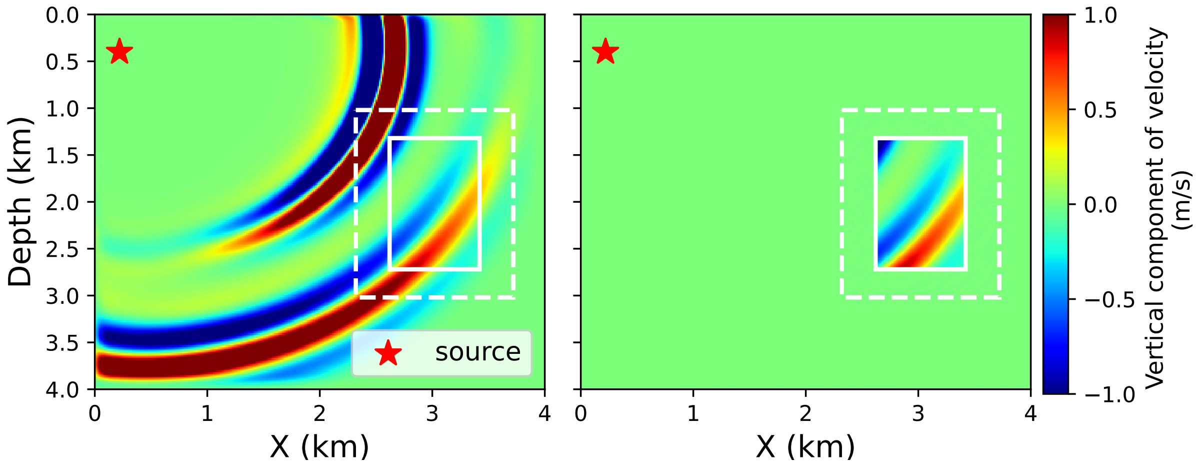

Figure 1. Left: full-model wave propagation simulation with a point source. Right: Target-oriented wave propagation using the Grid Injection Method (GIM). The colormap shows the snapshot of the vertical component of particle velocity during wave propagation. The red star represents the physical source. The white dashed and solid squares denote the localized absorbing boundary and grid injection sources, respectively.

requiring detailed knowledge of the background models outside the target region or source time functions. Synthetic experiments will demonstrate that the proposed amplitude-based tomography using multiple observables is resistant to the negative effects of non-repeatability and structural variations outside target area during time-lapse surveys, making it a promising and superior approach for high-resolution target-oriented inversion.

2 THEORY

2.1 Target-oriented waveform inversion

The target-oriented waveform inversion applied in this study was introduced by Yuan et al. (2017). It uses the Grid Injection Method (GIM) (Robertsson and Chapman, 2000; Borisov et al., 2015) as the local solver. GIM allows reconstructing a source expression on the surface of target regions, which serves as a localized forward modeling scheme and enables efficient calculation of synthetic seismograms after model alterations within a certain area. One example is shown in Figure 1, where we compare the full-model wave propagation simulation with localized simulation using GIM. The solid square serves as the injection source for local simulation, which is essentially the recorded boundary field. All forward and backward simulations will be conducted within the reduced absorbing boundary (the dashed white square shown in Figure 1).

On the receiver side, we can either use physical receivers in boreholes near the target region or create virtual receivers within the area of interest by extrapolating from physical receivers deployed on the Earth's surface or ocean bottom. By employing source-side GIM and receiver-side extrapolation, we can then perform full waveform inversion (FWI) in the target area, also known as target-oriented inversion, to quantify time-lapse changes. However, this localized inversion scheme relies on a key assumption: that baseline models are known beforehand and time-lapse changes are solely caused by structural alterations within the target region. This assumption may not always hold true, as structures outside the target area can also be affected by fluid injection and extraction. To mitigate errors caused by unknown external perturbations, a full-model FWI might be necessary before conducting target-oriented FWI, potentially reducing its appeal due to increased computational cost. Additionally, repeatability issues, such as changes in source-receiver positions, can also introduce errors into the target-oriented inversion scheme.

2.2 Seismic amplitude tomography

To address these challenges faced by target-oriented inversion and maintain its computational efficiency, we need to identify observables that are solely sensitive to changes in the target's immediate vicinity. While FWI is powerful because it inverts the entire waveform, including both amplitude and travel time information, for subsurface structures, travel times are inherently sensitive to the entire ray path. Conversely, amplitude information is primarily influenced by nearby structures. Given that, we proposed to apply the target-oriented inversion to some new observables, which are firstly defined in Fichtner and Igel (2009), including apparent S-wave velocity β_a:

$$\beta_a = \frac{A_v}{A_R}, \tag{1}$$

and apparent P-wave velocity α_a:

$$\alpha_a = \frac{A_v}{A_S}, \tag{2}$$

where A_v, A_R, and A_S denote the root-mean-square of windowed and/or filtered velocity, rotation, and strain signals, respectively. Rotational can be recorded by rotational sensors while strain can be recorded by strain meter or distributed acoustic sensing. The relative sensitivity density (kernel) of β_a and α_a with respect to S-wave (V_s) and P-wave (V_p) velocity, respectively, can be expressed as:

$$\beta_a^{-1}\delta_{V_s}\beta_a = \delta_{V_s}\ln\beta_a = \delta_{V_s}\ln A_v - \delta_{V_s}\ln A_R, \tag{3}$$

$$\alpha_a^{-1}\delta_{V_p}\alpha_a = \delta_{V_p}\ln\alpha_a = \delta_{V_p}\ln A_v - \delta_{V_p}\ln A_S. \tag{4}$$

Based on the above formulas, we can observe that the sensitivity of the combined amplitude-ratio observables to velocity structures is essentially equivalent to the sensitivity difference between translation and rotation, and sensitivity difference between translation and strain, respectively. This differential sensitivity theoretically cancels out the effects of the source and wave propagation, leading to sensitivity focused exclusively on the region near the receiver. To illustrate this further, we numerically calculated the sensitivity kernels of β_a and α_a under a constant background model. As shown in Figure 2, the top row displays the sensitivity kernels for translation, strain, and the combined apparent P-wave velocity amplitude (α_a) with respect to P-wave velocity. The bottom panel shows the same for translation, rotation, and apparent S-wave speed amplitude (β_a) with respect to S-wave velocity. Because we use amplitude-based observables, we will refer to the inversion of α_a and β_a as amplitude tomography, distinct from FWI and travel-time tomography.

3 SYNTHETIC EXPERIMENTS

3.1 Mitigating 4D repeatability issues

To verify the robustness and accuracy of the proposed target-oriented amplitude tomography, we will exemplarily invert the S-wave speed amplitude β_a and conduct two set of synthetic examples. First, we would like to check if the amplitude tomography can be immune to source positions errors which are typical repeatability issues we face in time-lapse surveys. We choose a surface-bore configuration, which is illustrated in Figure 3. The red stars represent the six physical point sources with spacing of 10 m. In total of six receivers with spacing of 10 m are deployed in the target region indicated by the black triangles, recording both translational and rotational motions. The time-lapse perturbation is shown on the left panel of Figure 3. We use a Ricker wavelet with dominant frequency of 4.5 Hz as the source wavelet and add it onto the vertical particle velocity component. We use time-domain finite-difference method to solve the 2D elastic wave equation. The S-wave velocity perturbation (ΔV_s) is estimated by iteratively minimizing the 2-norm difference between observed and modeled quantities for both translation and apparent S-wave velocity β_a.

Figure 4 presents the inversion results obtained using translation and the amplitude-ratio based β_a. The top panel shows the inverted shear-wave velocity change (ΔV_s) using translation (Figure 4b) and β_a (Figure 4c) for the case of true source locations (also known as repeated sources). The bottom panel shows the inverted ΔV_s using incorrect source positions (non-repeated sources). As evident from the figure, the target-oriented inversion based on the amplitude-ratio observable β_a is resistant to source location errors.

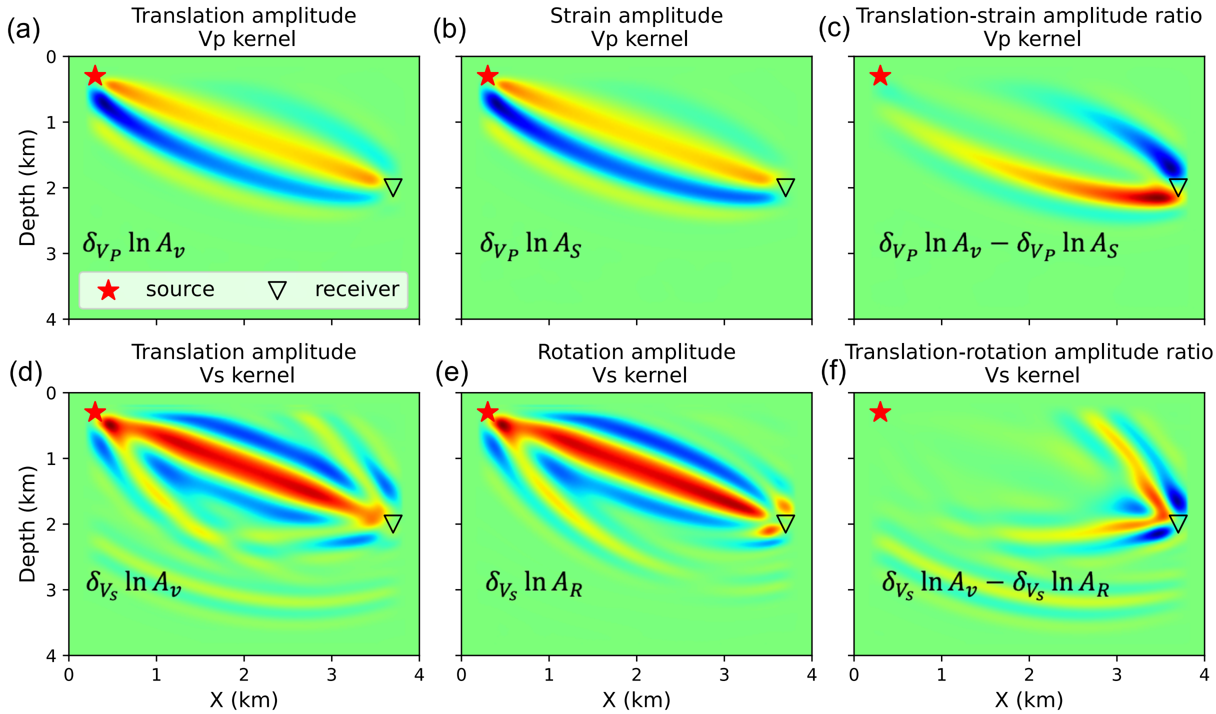

Figure 2. (a) – (c): The translation, strain, and the combined the apparent P-wave speed amplitude α_a sensitive kernels with respect to P-wave velocity. (d) – (f): The translation, rotation, and the combined the apparent S-wave speed amplitude β_a sensitive kernels with respect to S-wave velocity.

3.2 Mitigating effects of unknown perturbations outside target area

To further assess the effectiveness of the proposed target-oriented amplitude tomography, we introduce the scenario of unknown velocity perturbations outside the target area (Figure 5d). By comparing the inverted time-lapse perturbations without (Figure 5b, c) and with (Figure 5e, f) these unknown perturbations, we observe that the amplitude-ratio based observables are significantly less sensitive to velocity changes outside the receiver vicinity compared to conventional translational recordings.

4 DISCUSSION AND CONCLUSIONS

This study demonstrates the potential of applying new observables, like apparent P- and S-wave velocities, to target-oriented amplitude inversion. Our proposed method maintains the efficiency of target-oriented inversion while leveraging the near-receiver sensitivity of amplitude ratios. This makes model-driven local simulations more robust against baseline model errors. This method functions much like a magnifying glass, zooming in on a particular area while filtering out external influences. Furthermore, this concept extends beyond time-lapse surveys in exploration seismology. It can be applied to larger-scale structural inversions using multi-type waveforms. The combined observables in this study enable seismic tomography without relying on travel times. Consequently, the influence of travel paths, inaccurate source locations, and timing functions is significantly reduced, effectively mitigating non-repeatability issues common in time-lapse survey.

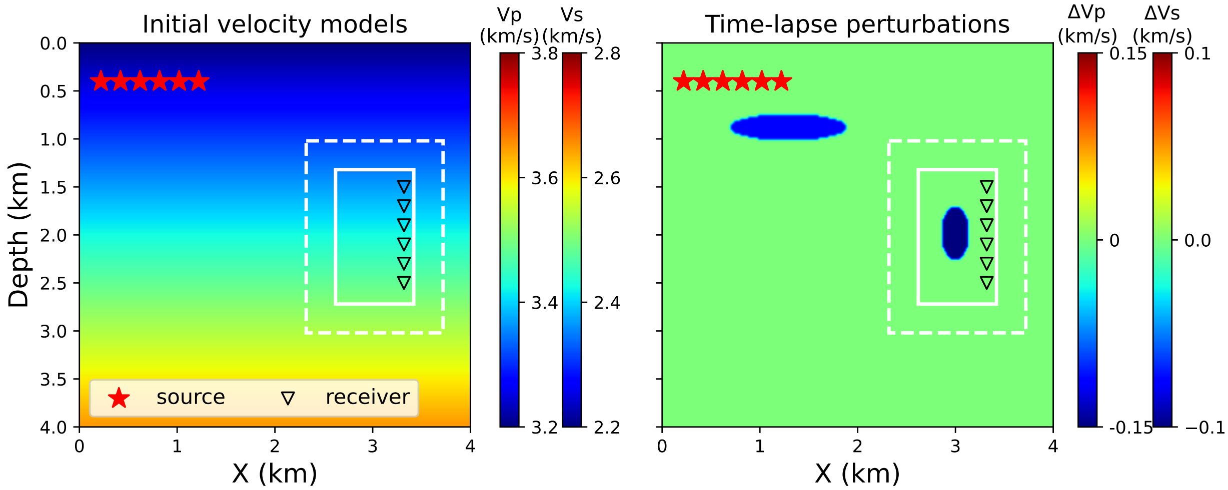

Figure 3. Baseline velocity models (left) and time-lapse perturbations (right) using a surface-borehole acquisition setup. This model is used throughout the synthetic examples in this study. The white squares covering the target area where we perform targeted inversion.

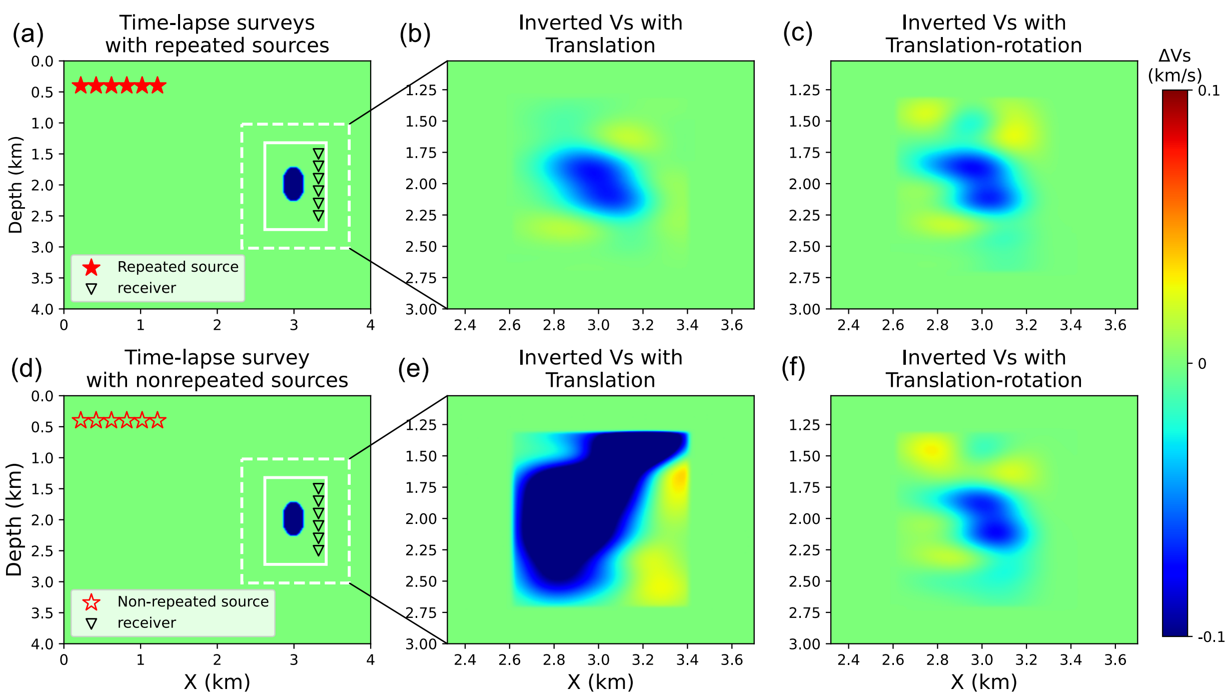

Figure 4. (a) True time-lapse V_s perturbation with repeatable sources. (b) Inverted time-lapse perturbation using target-oriented waveform inversion with only translational recordings (particle velocity) and assuming accurate source locations. (c) Same as (b) but using inverted apparent S-wave velocity (β_a). (d) True time-lapse V_s perturbation with inaccurate source locations (hollow stars). (e) Inverted time-lapse perturbation using only translational recordings (particle velocity) with inaccurate source locations. (f) Same as (e) but using apparent S-wave velocity (β_a) with inaccurate source locations. All inversions are performed using 20 iterations.

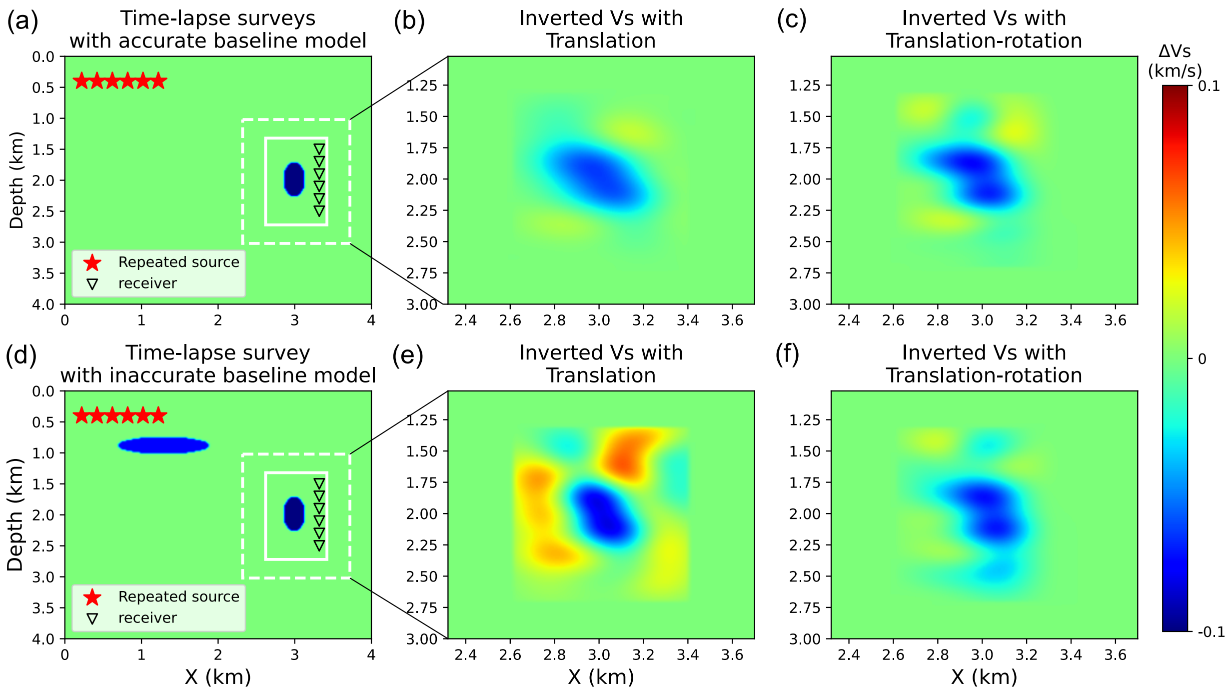

Figure 5. (a) True time-lapse V_s perturbation with accurate baseline models. (b) Inverted time-lapse perturbation using target-oriented waveform inversion with only translational recordings (particle velocity) and assuming accurate baseline models. (c) Same as (b) but using inverted apparent S-wave velocity (β_a). (d) True time-lapse V_s perturbation with inaccurate baseline models (unknown perturbations occurred outside the target area). (e) Inverted time-lapse perturbation using only translational recordings (particle velocity) with inaccurate source locations. (f) Same as (e) but using apparent S-wave velocity (β_a) with inaccurate baseline models. All inversions are performed using 20 iterations.

REFERENCES

Biondi, E., G. Barnier, B. Biondi, and R. G. Clapp, 2023, Target-oriented elastic full-waveform inversion through acoustic extended image-space redatuming: Geophysics, 88, R269–R296.

Borisov, D., S. C. Singh, and N. Fuji, 2015, An efficient method of 3-d elastic full waveform inversion using a finite-difference injection method for time-lapse imaging: Geophysical Journal International, 202, 1908–1922.

Fichtner, A., and H. Igel, 2009, Sensitivity densities for rotational ground-motion measurements: Bulletin of the Seismological Society of America, 99, 1302–1314.

Robertsson, J. O., and C. H. Chapman, 2000, An efficient method for calculating finite-difference seismograms after model alterations: Geophysics, 65, 907–918.

Willemsen, B., A. Malcolm, and W. Lewis, 2016, A numerically exact local solver applied to salt boundary inversion in seismic full-waveform inversion: Geophysical Journal International, 204, 1703–1720.

Yuan, S., N. Fuji, S. Singh, and D. Borisov, 2017, Localized time-lapse elastic waveform inversion using wavefield injection and extrapolation: 2-d parametric studies: Geophysical Journal International, 209, 1699–1717.

Yuan, S., N. Fuji, and S. C. Singh, 2021, High-frequency localized elastic full-waveform inversion for time-lapse seismic surveys: Geophysics, 86, R277–R292.

Zhou, W., and D. Lumley, 2021, Nonrepeatability effects on time-lapse 4d seismic full-waveform inversion for ocean-bottom node data: Geophysics, 86, R547–R561.